Biofabrication of Reduced Graphene Oxide using *Rhododendron micranthum* Turcz. Aqueous Leaf Extract and its Analgesia Efficiency and Local Anesthetic Effect

Huihong Xie,[a#] Yinjie Zheng,[a,#] Lishuang Chen,[b] Xiaonan Zhang,[c,*] and Ting Li [d,*]

[#] *Equal Contribution*
* *Corresponding author: fjslliting@126.com; xiaonanzhang0@hotmail.com*

DOI: 10.15376/biores.21.1.1429-1442

GRAPHICAL ABSTRACT

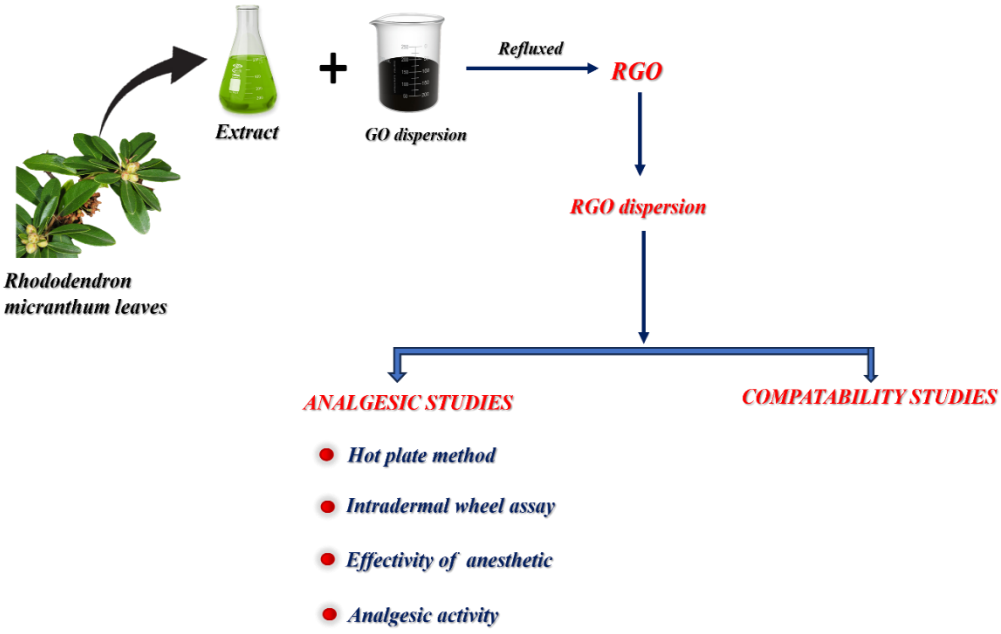

Biofabrication of Reduced Graphene Oxide Using *Rhododendron micranthum* Turcz. Aqueous Leaf Extract and its Analgesia Efficiency and Local Anesthetic Effect

Huihong Xie,[a,#] Yinjie Zheng,[a,#] Lishuang Chen,[b] Xiaonan Zhang,[c,*] and Ting Li [d,*]

The biosynthesis of Reduced Graphene Oxide (RGO) was shown using an aqueous leaf extract of *Rhododendron micranthum* Turcz. as a reductant by deoxygenation of Graphene Oxide (GO). The reduction of GO to RGO was shown as a shift in UV-Vis peak from 230 nm to 270 nm. X-ray diffraction (XRD), Fourier Transform Infrared Spectroscopy (FTIR), and Raman spectroscopy confirmed the GO reduction. Thermal gravimetry and zeta potential measurements exhibited the good stability of RGO. Transmission Electron Microscopy (TEM) results showed thin and transparent RGO sheets. Cell viability results showed that the mesenchymal stem cells (MSCs) of adult goats were viable in the presence of RGO at a concentration of 0.1 mg/mL, and their properties were retained. The analgesic effect of RGO was assessed in mice through the oral administration of different doses of RGO. Writhing episodes induced by acetic acid were decreased dose-dependently. Also, the inflammatory effect of RGO was shown by measuring the hind paw volume of rat exhibited the decreased inflammation with increased RGO concentration. The local anesthetic activity was assessed in guinea pig models and frog, revealing that the RGO exhibited a substantial local anesthetic effect in both the animals with decreased response in dose dependent manner.

DOI: 10.15376/biores.21.1.1429-1442

Keywords: RGO; MSCs; Mesenchymal stem cells; Rhododendron micranthum Turcz.*; Analgesia; Anesthesia*

*Contact information: a: Department of Anesthesiology, Shengli Clinical Medical College of Fujian Medical University, Fujian Provincial Hospital, Fuzhou University Affiliated Provincial Hospital; b: Fujian Medical University, Fuzhou, Fujian, China; c: Department of Anesthesia, Shijiazhuang Maternity & Child Healthcare Hospital, Shijiazhuang 050000, Hebei, China; d: Department of Radiology, Shengli Clinical Medical College of Fujian Medical University, Fujian Provincial Hospital, Fuzhou University Affiliated Provincial Hospital; #Equal Contribution; *Corresponding author: fjslliting@126.com; xiaonanzhang0@hotmail.com*

INTRODUCTION

In the medical domain, anesthesia refers to a state induced by medical means in which an individual, whether consciously or not, experiences a loss of control over specific body parts or the entire body, as well as a diminished awareness of their surroundings. This induced state can transiently result in numbness, paralysis, and amnesia (Fitz-Henry 2011; Goneppanavar and Prabhu 2013; Subrahmanyam and Mohan 2013; Gelb *et al.* 2018). Anesthesia functions by suppressing or temporarily ceasing the functioning of the central nervous system, thereby eliminating reactions and perceptions to outer stimuli. Anesthesia is characterized by amnesia and a state of unconsciousness (Ullah *et al.* 2014; Lewis *et al.* 2015; Mallinson 2019). The application

of anesthesia in medical procedures is essential for mitigating or eliminating pain, inducing muscle paralysis, and inducing amnesia and loss of consciousness.

Anesthesia in surgical settings is classified into three main groups, each with distinct uses, advantages, and disadvantages. The categories include global anesthesia, peripheral nerve anesthesia, and regional anesthesia (or local anesthesia). Patients do not have knowledge of the events happening, such as surgeries, and are rendered fully insensible during general anesthesia. Anesthesia of this kind is delivered either by means of inhaled gases and vapors using respiratory equipment or through intravenous techniques (Bandana Medhi *et al.* 2003; Klomp *et al.* 2012; Radvansky *et al.* 2015; Lu *et al.* 2021).

In the case of regional or local anesthesia, an anesthesiologist will administer spinal or epidural injections to desensitize specific areas of the body that require surgery. Patients can undergo these procedures while awake but sedated, thereby achieving a pain-free surgical experience. Spinal and epidural anesthesia are frequently used types of this anesthesia. Peripheral nerve anesthesia is the administration of an anesthetic directly into a targeted body region for minor surgical procedures (Subrahmanyam and Mohan 2013; Lewis *et al.* 2015; Mallinson 2019).

The selection of anesthesia is determined by various factors, such as the anesthesiologist's assessment, the patient's preference, medical history of the patient, and advice of the surgeon. Regional anesthesia is commonly used to numb a substantial portion, such as the lower half of the body (Klomp *et al.* 2012; Ullah *et al.* 2014; Lewis *et al.* 2015; Radvansky *et al.* 2015; Mallinson 2019). An anesthetic is administered by injection, either into the epidural space or spinal canal. This allows the patient to stay conscious but relaxed, often with the assistance of sedatives.

Epidural anesthesia, commonly administered for childbirth or orthopedic surgeries involving the lower body, entails the injection of an anesthetic into the epidural space, which is situated outside the spinal canal (Fitz-Henry 2011; Goneppanavar and Prabhu 2013; Subrahmanyam and Mohan 2013). Spinal anesthesia, administered directly into the spinal canal, is frequently employed for surgical procedures involving the lower extremities (Klomp *et al.* 2012; Ullah *et al.* 2014; Lewis *et al.* 2015; Radvansky *et al.* 2015; Mallinson 2019). Current developments in anesthesia focus on the exploration of anesthetic drugs that utilize nanotechnology. Studies have specifically investigated the properties of nanoparticles made from plant extracts, including their ability to act as local anesthetics, reduce inflammation, and provide pain relief (Bandana Medhi *et al.* 2003; Lu *et al.* 2011; Klomp *et al.* 2012; Ullah *et al.* 2014; Lewis *et al.* 2015; Radvansky *et al.* 2015).

Graphene-based compounds, particularly reduced graphene oxide (RGO), exhibit physiological effects due to their unique physicochemical properties (Chen *et al* 2018; Liu *et al* 2019; Liu S, and Zeng *et al* 2011). RGO nanosheets possess sharp edges and a high surface area, which can physically disrupt bacterial membranes, leading to cell lysis and death. Additionally, RGO has been shown to generate reactive oxygen species (ROS), contributing to oxidative stress in microbial cells and enhancing its antimicrobial efficacy (Mann *et al* 2021; Alayande *et al* 2020; Khalil *et al* 2020).

Beyond antimicrobial activity, graphene oxide (GO) and RGO may also influence pain signaling pathways. Their interaction with cellular membranes and proteins can modulate ion channels and inflammatory mediators. When paired with bioactive medicinal compounds, GO and RGO can act as carriers that enhance drug delivery, prolong retention time, and facilitate controlled release—thereby amplifying analgesic effects (Attia *et al.* 2021). RGO is a derivative that can be obtained from the

chemical or thermal reduction of GO (Gao 2015; Báez *et al* 2017; Navya Rani *et al* 2017).

Hydrazine, a reducing agent, chemically reduces graphene oxide (GO) and is widely acknowledged as the most successful way for synthesizing graphene. A drawback of this technique is the strong explosiveness and toxicity of the hydrated form of hydrazine. This necessitates the requirement of gentle conditions for the formation of graphene. Zhang *et al.* (2010) utilized a simple technique to produce graphene, employing L-Ascorbic acid as the reducing agent. Additionally, they determined the solubility of graphene in commonly used solvents such as N-dimethyl formamide, water, and N,N-methyl-2-pyrrolidone. Because RGO lacks the functional groups needed for solubility, a stabilizer becomes necessary to disperse it in aqueous solutions. The stabilizer typically contains surfactants or polymers that can interact with both RGO and water, thus maintaining a stable dispersion. Fernandez-Merino *et al.* (2010) and Ma *et al.* (2013) developed a stable dispersion of reduced graphene oxide (RGO) by utilizing carboxymethyl starch and L-Lysine as stabilizing agents. Given the extensive range of applications for graphene and the need for up-to-date techniques of preparing it, this study focused on the biosynthesis of RGO using plant extracts (Jin *et al.* 2021; Dominic *et al.* 2022). Several plants have been already used for reduction of GO to obtain an aqueous soluble RGO.

In the present work, the authors showed the green synthesis of RGO using *Rhododendron micranthum* Turcz. aqueous leaf extract as a reductant through the deoxygenation of GO. The obtained RGO was studied using various spectroscopic and microscopic techniques. Additionally, the analgesic effect of RGO was assessed in mice through oral administration of different doses of RGO. The occurrence of writhing episodes induced by acetic acid decreased dose-dependently. Similarly, RGO's local anesthetic activity was assessed in guinea pig models and frog, revealing that the RGO exhibited substantial local anesthetic effects in both animals.

Testing RGO in amphibians, such as frogs, offers a novel approach to evaluating its biocompatibility in aquatic environments—an important consideration in nanomaterial safety. Unlike conventional studies focused on mammals, this work explored RGO's local anesthetic effects in non-mammalian models, providing new insights with both biomedical and ecological relevance. This amphibian-based evaluation expands the scope of graphene-related pharmacological research and highlights its potential for broader biological applications.

EXPERIMENTAL SECTION

Materials

Sulphuric acid (H_2SO_4), potassium bromide (KBr), graphite powder (99%), sodium nitrate ($NaNO_3$), hydrogen peroxide (H_2O_2), potassium permanganate ($KMnO_4$), acetic acid (CH_3COOH), hydrochloric acid (HCl), and other chemicals used in this study were of analytical grade. All the chemicals and solvents used in this study were purchased from Sigma Aldrich, Shanghai.

RGO Synthesis

The GO was produced by modifying the Hummers method using natural graphite flakes as the starting material (Perera *et al.* 2012). At first, 0.5 g of graphite flakes and an equivalent quantity of $NaNO_3$ were combined in 23 mL of concentrated H_2SO_4 (12.1 M, 98% purity). The mixture was subjected to magnetic stirring for a

duration of 15 min, while ensuring that the temperature remained within the range of 0 to 5 °C. Afterwards, a total of 4 g of $KMnO_4$ were slowly added to the mixture, taking care to maintain a temperature below 20 °C. The mixture was thereafter agitated for a duration of 90 min at 40 °C temperature within a water bath. During vigorous agitation for a duration of 10 min, 50 mL of double distilled water was introduced, which led to the formation of a suspension in dark brown color.

The suspension was subjected to additional processing by gradually introducing 6 mL of 30% H_2O_2 solution, followed by further dilution with 50 mL of double distilled water. To eliminate surplus manganese salts, the GO nanomaterial obtained was subjected to multiple washes using deionized water until a neutral pH was attained. The last stage entailed spreading the refined GO in water at 1 mg/mL of concentration. The dispersion was thereafter exposed to ultrasonication in an ultrasonic bath for roughly 3 h to accomplish exfoliation. The stable dispersion obtained was set aside for future experimental use.

Initially, 100 g of sunlight dried *R. micranthum* Turcz. Leaves were collected and made into powder form using a mortar and pestle. Then, 100 mL of double distilled water was added to about 1 g of obtained powder and boiled for 1 h in a water bath and filtered to obtain a clear extract solution using cellulose nitrate filter paper. To achieve stability of the suspension, GO (0.18 g) with 360 mL of double-distilled water were sonicated for half an hour. Then, 90 mL of filtered *R. micranthum* extract was used to treat the obtained stabilized suspension that was then refluxed. An aliquot of 90 mL filtered *R. micranthum* extract was added to above GO dispersion and refluxed. The color change was observed from light brown to black precipitate confirming the synthesis of RGO.

Characterization of RGO

UV-Visible spectroscopy

UV-Visible spectroscopy was performed using a Jasco V-670 UV-Vis double beam spectrophotometer (JASCO, Tokyo, Japan). The *Rhododendron micranthum* sample underwent a process of drying followed by dispersion in double-distilled water. The spectrum study was conducted using double distilled water as a reference blank.

Fourier transform infrared spectroscopy

A JASCO FTIR 4100 instrument (JASCO, Tokyo, Japan) was used to perform Fourier transform infrared (FTIR) spectroscopy in the range from 4000 to 400 cm^{-1}, with a resolution of 4 cm^{-1} in diffuse reflectance mode. The preparation of samples for this examination involved the combination of powdered plant extract and KBr powder, followed by compression into pellets.

X-ray diffraction

A Bruker D8 Advance diffractometer (Bruker, Karlsruhe, Germany) equipped with Cu Kα radiation (λ = 1.54 A°) was used to conduct X-ray diffraction (XRD) measurements at room temperature. The diffraction angles (2θ) ranged between 3 and 80°, with a step size of 0.02° and a scanning rate of 4° per min.

Raman spectroscopy

The Raman spectroscopy analysis was conducted using a Senterra R200-L equipment manufactured by Bruker Optics (Karlsruhe, Germany). The spectra were obtained by applying 532 nm wavelength of laser beam.

Transmission electron microscopy

The JEOL-2100 F electron microscope (JEOL, Tokyo, Japan) was used to obtain transmission electron microscopy (TEM) images, operating at 200 kV. To prepare the samples, desiccated plant extract was dispersed in water at 1 mg/mL concentration using ultrasonic settings. Afterwards, a little amount of this mixture was applied onto a Lacey carbon coated copper grid and subjected to vacuum drying.

Viability, Isolation, and Adhesion of Goat Adipose Tissue-derived MSCs (AdMSCs) on the RGO

The present investigation utilized MSCs obtained from adipose tissue of goats, as previously detailed (Elkhenany *et al.* 2016). An *in-vitro* assessment of cell viability and adhesion was conducted for a duration of 10 days using MTS (3-(4,5-dimethylthiazol-2-yl)-5-(3-carboxymethoxyphenyl)-2-(4-sulfophenyl)-2H-tetrazolium) analysis (Promega). The properties were subsequently verified on the 7th day using propidium iodide (PI) dye (Invitrogen) and calcein-AM dye (Invitrogen) under a microscope. Goat AdMSCs were seeded onto a 24-well plate coated with RGO at a density of 1.0×10^3 cells per well. The cells were stained and viewed using a Zeiss Axiovert microscope (Carl Zeiss) with a DS-Qi1Mc Nikon Digital Sight camera, following the manufacturer's guidelines. The AdMSCs were evenly distributed over both surfaces of RGO and polystyrene simultaneously for the purpose of comparison.

Analgesic Studies

In vivo design

This study involved the use of Dunkin Hartley *Cavia porcellus* (breed guinea pigs), frogs of any gender, and adult male albino mice. The present animal research was carried out in line with the principles and standards outlined in the institutional Ethical Committee of Animal Experimentation (Approval number: 2022-07-05). All the animal experiments were performed according to ethical committee guidelines of Shengli Clinical Medical College of Fujian Medical University, Fujian Provincial Hospital, Fuzhou University Affiliated Provincial Hospital.

Based on the dose of RGO (40, 20, 10, 5, and 0 mg/kg), male albino mice were divided into five groups for the analgesic activity assay. Each group consisted of 10 animals. After treatment for 90 min, an intraperitoneal injection of 0.6% CH_3COOH at a dose of 100 mg/kg was given to mice. Subsequent observations were conducted for a duration of 20 min to document the frequency of writhing behavior. During the hot plate assay, mice were laid down on a hot plate that was maintained at a constant temperature of 55 ± 0.5 °C. The authors quantified the latency period, which refers to the time interval between placing the mouse on the plate and the onset of irritation in its feet, by employing a stopwatch.

In preparation for the intradermal wheal assay, the back hair of guinea pigs was depilated. Following the confirmation of their typical reaction to pin pricks, a volume of 0.2 mL of RGO was administered intradermally on the left side of the back, while an equal amount of 0.9% normal saline was supplied on the right side. Ink was used to demarcate the injection locations. Pin pricks were administered at regular intervals of

2 to 3 s and repeated for every 5 min. The absence of any squeal reaction to all five pricks indicated a favorable anesthetic effect.

To assess the effectiveness of a local anesthetic, the brain of a frog was removed, the upper part of its spinal cord damaged, and a surgical cut was performed on its side to create a space for administering the medication solution. The frog's leg was suspended and exposed to a 0.05 N HCl solution to evaluate the reflex withdrawal. Finally, to evaluate the anti-inflammatory effects, a rat's hind paw was submerged in water up to the lateral malleolus. Once the water level was established, the paw volume was measured using a micropipette. Subsequently, carrageenan, a well-established inflammatory substance, was inserted beneath the sole surface of the right hind paw.

This research was carried out in line with the principles and standards outlined in the institutional Committee on Ethics of Animal Experimentation. All the animal experiments were performed according to ethical committee guidelines of Shengli Clinical Medical College of Fujian Medical University, Fujian Provincial Hospital, Fuzhou University Affiliated Provincial Hospital.

Statistical Analysis

The results are expressed as Mean ± Standard Deviation. The SPSS software (IBM, 10th version, Chicago, IL, USA) was used to perform all the statistical analyses. Analysis was done in triplicate. Mean values were used for statistical analysis. The p values ≤ 0.05 were taken as statistically significant.

RESULTS AND DISCUSSION

The concentration and electrical characteristics of RGO are frequently determined using UV-Vis spectroscopy. Specifically, it helps in identifying absorbance peaks that correspond to electronic transitions in the RGO. These peaks provide valuable information about the structure and functional groups present in the material. The mixture of GO and an aqueous extract of *Rhododendron micranthum* Turcz. was subjected to continuous reflux for approximately 10 h. After a duration of 6 h, the suspension, originally exhibiting a brown hue, underwent a transformation to a black coloration and then formed a precipitate. The UV-Vis spectrum exhibited an absorbance peak of GO at a wavelength of 234 nm, indicating the occurrence of a π–π^* transition in the aryl carbon – carbon bonds. The presence of a peak at 274 nm in the absorption spectrum of RGO suggests that the reduction of GO had occurred (Fig. 1). The observed red shift was used as a tool for reducing the gravitational pull of objects (GO).

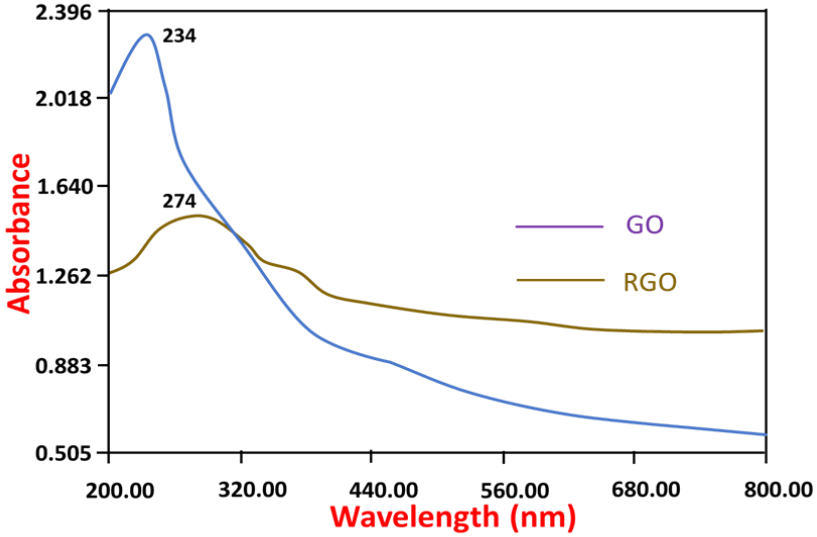

Fig. 1. UV–Visible spectra of GO and biofabricated RGO with peaks observed at 234 nm and 274 nm

Figure 2 shows the FTIR spectra of RGO and GO. The peaks seen at 1,610 cm^{-1} and 1,720 cm^{-1} in GO corresponded to the presence of aromatic and carbonyl groups, respectively. The absence of carbonyl peaks in the FTIR spectrum of RGO suggested the reduction of GO.

The XRD analysis of GO revealed a prominent and well-defined peak at 9.758º, indicating the presence of Bragg's reflection from the (002) plane. This reflection corresponds to an interlayer distance of 7.6 Aº (as shown in Fig. 3A). After reducing GO, a peak was observed in the XRD analysis at an angle of 26º, which corresponds to Bragg's reflection of the (001) plane. Additionally, the disappearance of a peak at 9.758º verifies the production of graphene.

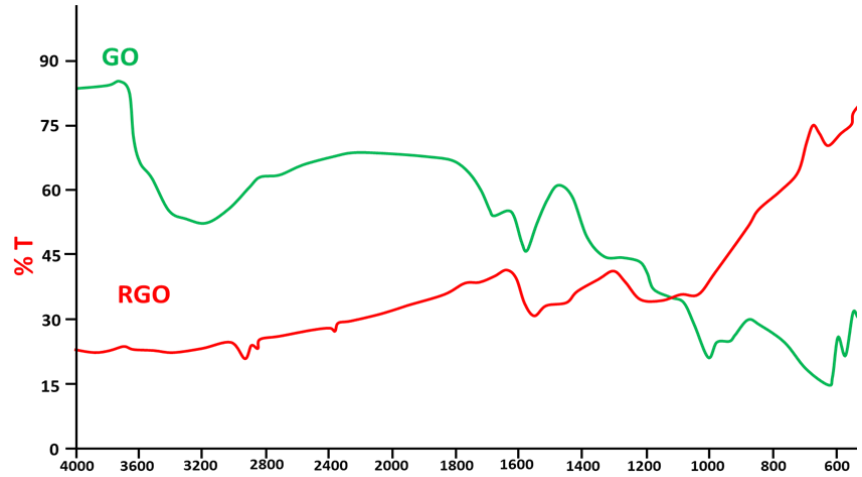

Fig. 2. FTIR spectrum of GO and biofabricated RGO with peaks seen at 1,610 cm^{-1} and 1,720 cm^{-1}

A Raman spectrum of graphene produced utilizing the aqueous *R. micranthum* Turcz. extract is shown in Fig. 3B. The most prominent features of graphene are the presence of the G peak at 1,580 cm^{-1} and a band identified as G at 2,700 cm^{-1}. The appearance of the G peak in graphene is due to the doubly degenerate E2g mode and the second-order phonons in the boundary zone, known as 2D or G´. The G' band is

typically absent in Raman spectra of defect-free graphite. The D peak was the highest rise at 1,350 cm^{-1} caused by these phonons. The presence of the G and D bands was revealed by the peak observed at 1,594 and 1,350 cm^{-1}, as shown in Fig. 3B. The absence of a 2D peak in the Raman spectra indicates a distinction between single-layered and few-layered graphene production.

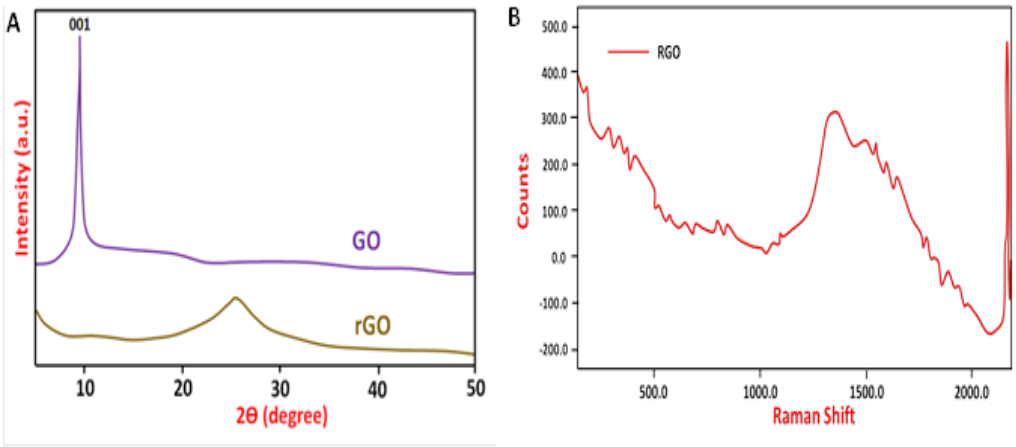

Fig. 3. (A) XRD pattern of RGO and GO well-defined peak at 9.758º and 26º; (B) Raman spectra of RGO with peak at 1,580 cm^{-1}

The TEM images of RGO are presented in Fig. 4. The TEM images revealed stacked layers of graphene (Fig. 4A). Figure 4B clearly depicts the graphene crystal planes as smooth and folded structures, exhibiting some little wrinkling. The folding process is dependent on the presence of hydrogen and partial chemical connections between layers. Therefore, the graphene produced in this work may consist of a small number of layers, ranging from one to a few.

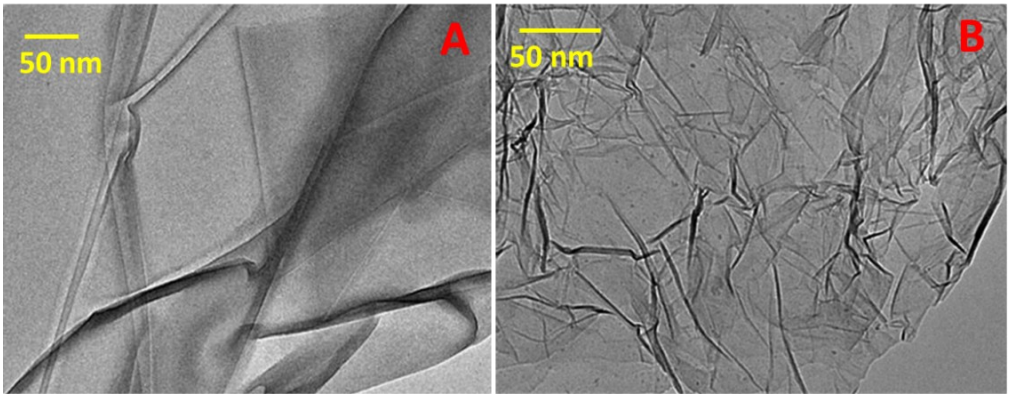

Fig. 4. (A) HR-TEM images of GO with stacked layers of graphene and (B) RGO with graphene crystal planes as smooth and folded structures

Evaluation of Biocompatibility

The cell survival of goat AdMSCs, which were first isolated, described, and cryopreserved, was evaluated *in vitro* using RGO films. The MTS proliferation assay was employed for this purpose (Elkhenany *et al.* 2015). The viability of MSCs was preserved and their ability to multiply was maintained on RGO films, which exhibited similar characteristics to a surface covered with polystyrene (Fig. 5A). Subsequently, the viability of the cells was verified using fluorescent dead-live labeling, as depicted in Fig. 5B. Through employing calcein-AM dye, which emits green fluorescence, it was determined that the cells adhere to the graphene films and maintain their vitality.

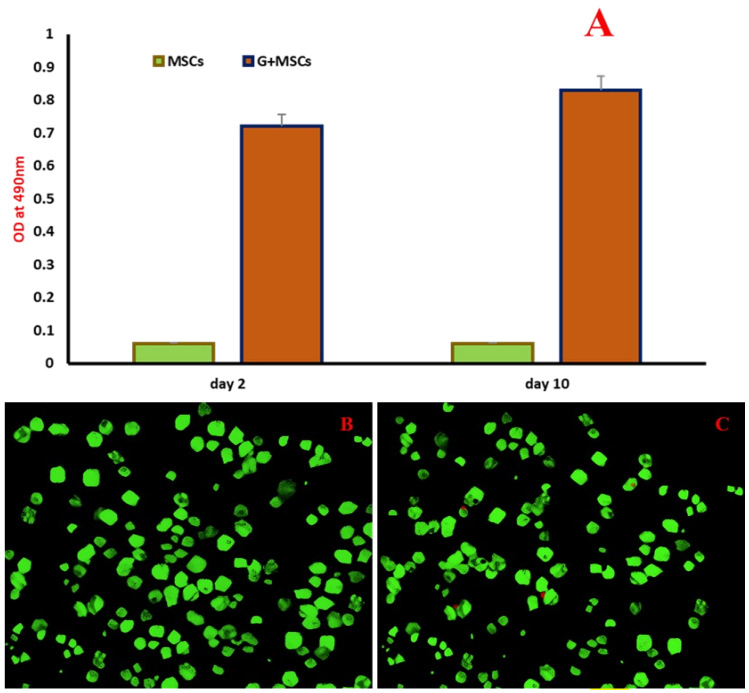

Fig. 5. (A) Cell viability examination by assay of MTT; (B) and (C) live-dead fluorescent staining showed undetectable levels of cell apoptosis were recorded by red PI staining

Analgesic Studies

The fall in writhing episodes in response to different doses of RGO is shown in Fig. 6A and 6B. These figures demonstrate a decrease in writhing episodes from the control group (RGO 0) to the highest dosage (RGO 40). Figure 7A illustrates the influence of RGO on the average inflammatory measurement (in mm) in mice. An observed pattern of diminishing inflammation was observed as the concentration of RGO increased, with the lower concentration showing the increased level of inflammation and *vice versa*.

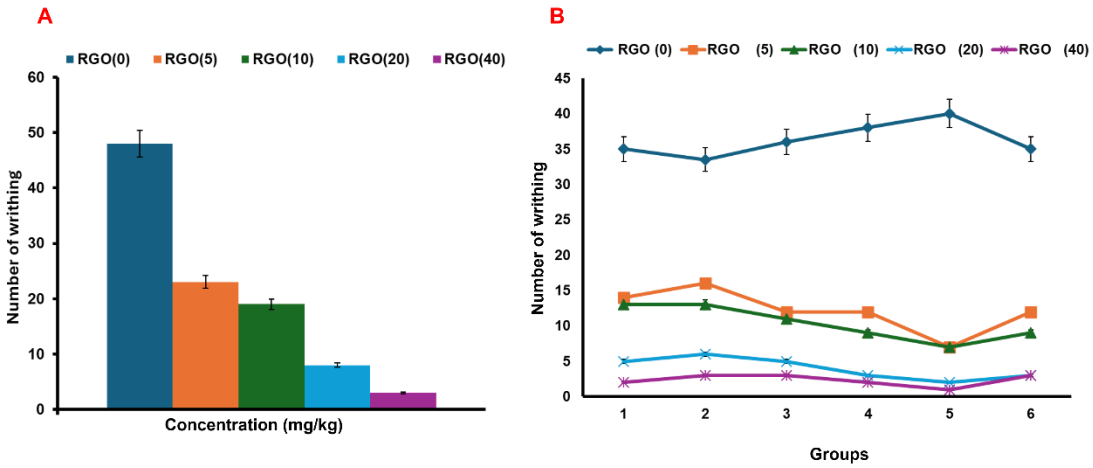

Fig. 6. Decrease in number of writhing with increased concentration of RGO; (A) Mean of writhing syndrome (number) in mice; (B) Acetic acid-induced writhing syndrome in mice by the effect of RGO

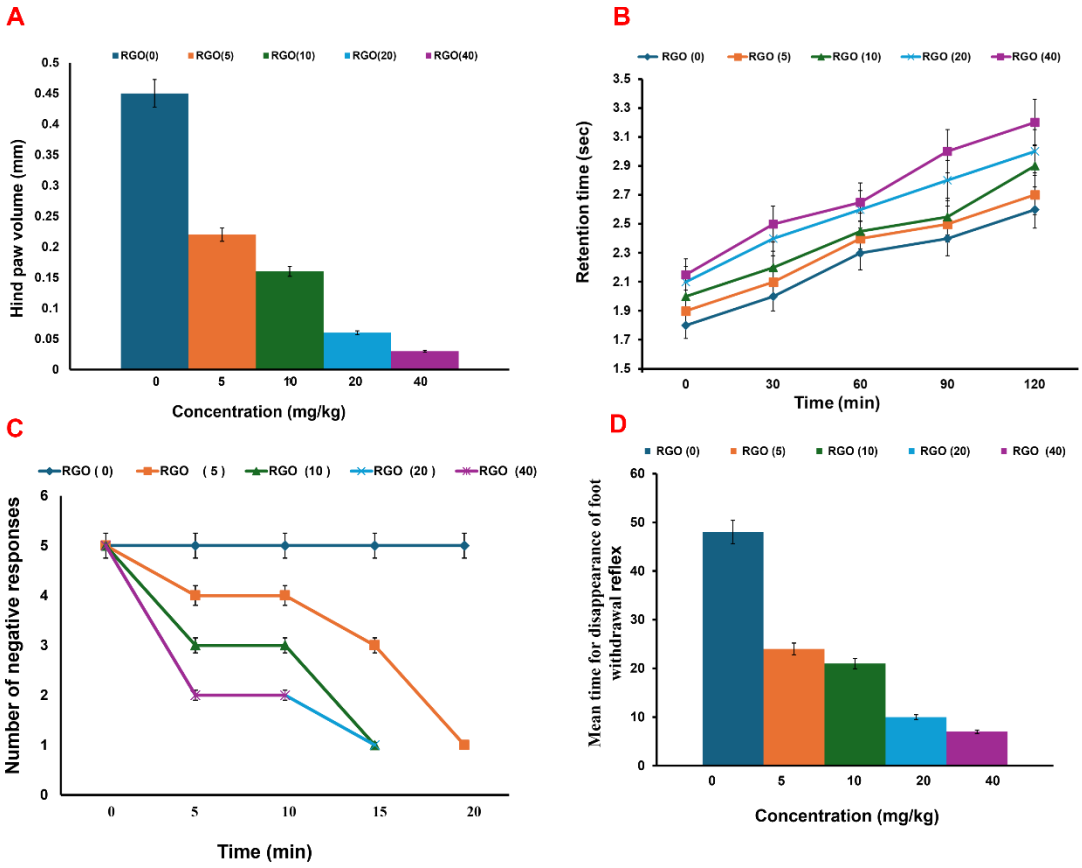

Fig. 7. Reduced activity was observed with increased concentration of RGO: (A) Mean of inflammation (mm) in rats; (B) Analgesic activity exhibited by RGO in albino mice hot plate method; (C) Intradermal wheal in left side of guinea pig; (D) Foot withdrawal reflex of frog by the effect of RGO

At a dosage of up to 40 mg/kg, RGO did not exhibit any appreciable pain-relieving properties according to the criteria applied to assess the effects. Significantly, in all groups including the control group reaction times at 60, 90, and 120 min gradually increased. The rise in sensitivity observed in the mice can be attributed to their reduced sensitivity to repeated subjection to the hot plate (Fig. 7B). The initiation of local anesthetic effects in guinea pigs using the intradermal wheal method was consistently detected at 20 min for all dosages of RGO (as shown in Fig. 7C). Figure 7D provides a detailed account of the impact of RGO on the automatic foot withdrawal in frogs that clearly demonstrates a decrease in the responsiveness of the reflex, from (RGO 0) to (RGO 40).

The evident analgesic effect revealed by chemical analysis indicated that the plants may have a similar function to non-narcotic pain relievers, which is consistent with the findings of Dastur (1948), who recorded the utility of plants for treating earaches and headaches through oral application (Witkin *et al.* 1952). Nevertheless, the extract exhibited no response to temperature stimulation. Similarly, a correlation was found between the dosage and the ability to reduce inflammation in mice with carrageenan-induced paw swelling (Dastur 1948). This finding supports the previous on the effectiveness of orally administered plant extracts in relieving pain and reducing fever, gout, and rheumatism (Kirtikar 1953; Rauf *et al.* 2017; Aktar *et al.* 2024; Kciuk *et al.* 2024). Dastur (1948) also observed the utilization of the newly harvested root in the treatment of persistent rheumatism, gout, edema, and recurring fever. The local anesthetic effectiveness of the plant was additionally confirmed using a standardized

approach, demonstrating substantial activity of the methanol extract derived from the root bark in the treated animals (Witkin *et al.* 1952).

Future Work

While the study has presented promising evidence for the analgesic and local anesthetic potential of RGO synthesized *via* a green route, further investigation is essential to ensure its safety and efficacy. Future work should focus on comprehensive toxicological assessments to determine whether the formulated RGO exhibits any cytotoxic, genotoxic, or immunogenic effects in both *in vitro* and *in vivo* models. Additionally, it is crucial to delineate the role of excipients such as CMC in the observed biological responses, as their presence may confound the interpretation of RGO's pharmacological activity. Controlled studies isolating the effects of RGO from those of CMC will help clarify this. Optimization of the formulation including particle size, surface functionalization, and delivery method should also be explored to enhance therapeutic outcomes while minimizing potential risks. These steps will be vital in advancing RGO-based materials toward safe and effective biomedical applications

CONCLUSIONS

1. This study demonstrated the environmentally friendly synthesis of reduced graphene oxide (RGO) through a sustainable approach. The deoxygenation of graphene oxide (GO) was facilitated by the utilisation of *Rhododendron micranthum* Turcz. leaf extract as a reducing agent. This sustainable approach conveys the possibilities of environmentally friendly techniques in nanomaterial synthesis, removing the necessity for harmful chemicals while ensuring effective RGO production. Fourier transform infrared (FTIR), Raman, and X-ray diffraction (XRD) results confirmed the deoxygenation GO to RGO. Transmission electron microscopy (TEM) images revealed the stacked layers of thin and transparent graphene sheets
2. In the presence of RGO at 0.1 mg/mL concentration, the MSCs of adult goats were viable and their properties were retained as stem cells.
3. The analgesic effect was assessed in mice through oral administration of different doses of RGO. The occurrence of writhing episodes induced by acetic acid was decreased dose-dependently.
4. The activity of regional anesthetic was assessed in guinea pig models and frog, revealing that the RGO exhibited substantial local anesthetic effects in both animals.
5. The prepared RGO appears to have potential in the future, exhibiting analgesic and local anesthetic properties.

Conflict of Interest

Authors have declared that no conflict of interest is associated with this work.

Funding

This work was supported by the Startup Fund for scientific research, Fujian Medical University (2022QH1303) and the General Project of Fujian Provincial

Education Department Middle-aged and Young Teachers Research Project (JAT241007).

Data Availability

The data associated with the findings of this study are available from the corresponding authors, upon reasonable request.

Ethical Statement

This research was carried out in line with the principles and standards outlined in the institutional Committee on Ethics of Animal Experimentation. All the animal experiments were performed according to ethical committee guidelines of Shengli Clinical Medical College of Fujian Medical University, Fujian Provincial Hospital, Fuzhou University Affiliated Provincial Hospital.

REFERENCES CITED

Aktar, M. A., Bhuia, M. S., Molla, S., Chowdhury, R., Sarkar, C., Shahriar, M. A., Reiner, Z., Sharifi-Rad, J., Calina, D., Shakil, M. A. K., *et al.* (2024). "Pharmacological and phytochemical review of *Acmella oleracea*: A comprehensive analysis of its therapeutic potential," *Discover Applied Sciences* 6, article 412. https//doi.org/10.1007/s42452-024-06108-5

Alayande, A. B., Obaid, M., and Kim, I. S. (2020). "Antimicrobial mechanism of reduced graphene oxide-copper oxide (rGO-CuO) nanocomposite films: The case of *Pseudomonas aeruginosa* PAO1," *Mater. Sci. Eng. C* 109, article 110596. https://doi.org/10.1016/j.msec.2019.110596

Attia, M. S., El-Sayyad, G. S., Abd Elkodous, M., Khalil, W. F., Nofel, M. M., Abdelaziz, A. M., Farghali, A. A., El-Batal, A. I., and El Rouby, W. M. A. (2021). "Chitosan and EDTA conjugated graphene oxide antinematodes in eggplant: Toward improving plant immune response," *Int. J. Biol. Macromol*. 179, 333-344. https://doi.org/10.1016/j.ijbiomac.2021.03.005

Bandana Medhi, H. N., Khanikor, L. C., Lahon, P. M., and Barua, C. (2003). "Analgesic, antiinflammatory and local anaesthetic activity of *Moringa pterygosperma* in laboratory animals," *Pharm. Biol*. 41(4), 248-252. https//doi.org/10.1076/phbi.41.4.248.15670

Báez, D. F., Pardo, H., Laborda, I., Marco, J. F., Yáñez, C., and Bollo, S. (2017). "Reduced graphene oxides: Influence of the reduction method on the electrocatalytic effect towards nucleic acid oxidation nanomaterials," *Nanomaterials* 7(7), article 168. https://doi.org/10.3390/nano7070168

Chen, C., Gan, Z., Zhou, K., Ma, Z., Liu, Y., and Gao, Y. (2018). "Catalytic polymerization of N-methylthionine at electrochemically reduced graphene oxide electrodes," *Electrochim. Acta* 283, 1649-1659.

Dastur, J. F. (1948). "Medicinal plants of India and Pakistan," in: *Treasure House of Books*, Taraprevala Sons and Co. Ltd., Bombay, India, pp. 160-163.

Dominic, R. M., Punniyakotti, P., Balan, B., and Subramaniah, A. (2022). "Green synthesis of reduced graphene oxide using *Plectranthus amboinicus* leaf extract and its supercapacitive performance," *Bull. Mater. Sci.* 45, article 2. https://doi.org/10.1007/s12034-021-02580-6

Elkhenany, H., Amelse, L., Caldwell, M., Abdelwahed, R., and Dhar, M. (2016). "Impact of the source and serial passaging of goat mesenchymal stem cells on osteogenic differentiation potential: Implications for bone tissue engineering," *J. Anim. Sci. Biotechnol*. 7, 1-13. https://doi.org/10.1186/s40104-016-0074-z

Elkhenany, H., Amelse, L., Lafont, A., Bourdo, S., Caldwell, M., and Neilsen, N. (2015). "Graphene supports *in vitro* proliferation and osteogenic differentiation of goat adult mesenchymal stem cells: Potential for bone tissue engineering," *J. Appl. Toxicol*. 110, 367-374. https://doi.org/10.1002/jat.3024

Fernandez-Merino, M. J., Guardia, L., Paredes, J. I., Villar-Rodil, S., Solis-Fernandez, P., and Martinez-Alonso, A. (2010). "Vitamin C is an ideal substitute for hydrazine in the reduction of graphene oxide suspension," *J. Phys. Chem*. *C* 114(14), 6426-6432. https://doi.org/10.1021/jp100603h

Fitz-Henry, J. (2011). "The ASA classification and peri-operative risk," *Ann. R. Coll. Surg. Engl*. 93(3), 185-217. https://doi.org/10.1308/147870811X565070a

Gao, W. (2015). "The chemistry of graphene oxide," in: *Graphene Oxide*, pp. 61-95.

Gelb, A. W., Morriss, W. W., Johnson, W., Merry, A. F., Abayadeera, A., and Belii, N. (2018). "World Health Organization – World Federation of Societies of Anaesthesiologists (WHO-WFSA) international standards for a safe practice of anesthesia," *Anesth. Analg.* 126(6), 2047-2055. https://doi.org/10.1213/ANE.0000000000002927

Goneppanavar, U., and Prabhu, M. (2013). "Anaesthesia machine: Checklist, hazards, scavenging," *Ind. J. Anaes.* 57 (5), 533-540. https://doi.org/10.4103/0019-5049.120151

Jin, Y., Xianmin, X., Kai, H., Mengyu, Z., Shu, Q., Min, L., and Lile, W. (2021). "Green synthesis of reduced graphene oxide (RGO) using the plant extract of *Salvia spinosa* and evaluation of photothermal effect on pancreatic cancer cells," *Journal of Molecular Structure* 0022-2860(1245), article 131064. https://doi.org/10.1016/j.molstruc.2021.131064

Kciuk, M., Garg, A., Rohilla, M., Chaudhary, R., Dhankhar, S., Dhiman, S., Bansal, S., Saini, M., Singh, T. G., Chauhan, S., *et al.* (2024). "Therapeutic potential of plant-derived compounds and plant extracts in rheumatoid arthritis—Comprehensive review," *Antioxidants* 13(7), article 775. https://doi.org/10.3390/antiox13070775

Kirtikar, K. R. (1933). *The Indian Materia Medica*, Vol. 1, 2nd Ed., Antiquarian and valuable Book Sellers, Kumara, Calcutta, India, pp. 810-816.

Klomp, T., Van Poppel, M., Jones, L., Lazet, J., Di Nisio, M., and Lagro-Janssen, A. L. (2012). "Inhaled analgesia for pain management in labour," *Cochrane Db. Syst. Rev.* 12(9), article CD009351. https://doi.org/10.1002/14651858.CD009351.pub2

Khalil, W. F., El-Sayyad, G. S., El Rouby, W. M. A., Sadek, M. A., Farghali, A. A., and Batal, I. El A. (2020). "Graphene oxide-based nanocomposites (GO-chitosan and GO-EDTA) for outstanding antimicrobial potential against some *Candida* species and pathogenic bacteria," *Int. J. Biol. Macromol*. 164, 1370-1383.

Lewis, S. R., Price, A., Walker, K. J., McGrattan, K., and Smith, A. F. (2015). "Ultrasound guidance for upper and lower limb blocks," *Cochrane Db. Syst. Rev.* 9, article CD006459. https://doi.org/10.1002/14651858.CD006459.pub3

Liu, Y., Song, N., Ma, Z., Zhou, K., Gan, Z., Gao, Y., Tang, S., and Chen, C. (2019). "Synthesis of a poly(N-methylthionine)/reduced graphene oxide nanocomposite for the detection of hydroquinone," *Mater. Chem. Phys*. 223, 548-556.

Liu, S., Zeng, T. H., Hofmann, M., Burcombe, E., Wei, J., Jiang, R., Kong, J., and Chen, Y. (2011). "Antibacterial activity of graphite, graphite oxide, graphene

oxide, and reduced graphene oxide: Membrane and oxidative stress," *ACS Nano* 5, 6971-6980.

Lu, Y., Wan, X., Li, L., Sun, P., and Liu, G. (2021). "Synthesis of a reusable composite of graphene and silver nanoparticles for catalytic reduction of 4- nitro phenol and performance as anti-colorectal carcinoma," *J. Mater. Res. Technol*. 12, 1832-1843. https://doi.org/10.1016/j.jmrt.2021.03.093

Ma, J., Wang, X., Liu, Y., Wu, T., Liu, Y., Guo, Y., Li, R., Sun, X., Wu, F., Lia, C., *et al.* (2013). "Reduction of graphene oxide with Llysine to prepare reduced graphene oxide stabilized with polysaccharide polyelectrolyte," *J. Mater. Chem. A* 1, 2192-2201. https://doi.org/10.1039/C2TA00340F

Mallinson, T. (2019). "*Fascia iliaca* compartment block: A short how-to guide," *Journal of Paramedic Practice* 11(4), 154-215. https://doi.org/10.12968/jpar.2019.11.4.154

Mann, R., Mitsidis, D., Xie, Z., McNeilly, O., Ng, Y. H., Amal, R., and Gunawan, C. J. (2021). "Antibacterial activity of reduced graphene oxide," *Nanomater*. 2021, article 9941577.

Navya Rani, M., Ananda, S., and Rangappa, D. (2017). "Preparation of reduced graphene oxide and its antibacterial properties," *Mater. Today* 4, 12300-12305.

Perera, S. D., Mariano, R. G., Nijem, N., Chabal, Y. J. P., Ferraris, J. P., and Balkus, K. J. J. (2012). *Power Sources* 215, 1-10. https://doi.org/10.1016/S0378-7753(12)01135-4

Radvansky, B. M., Shah, K., Parikh, A., Sifonios, A. N., Le, V., and Eloy, J. D. (2015). "Role of ketamine in acute postoperative pain management: A narrative review," *Biomed. Res. Int*. 2015(1), article 749837. https://doi.org/10.1155/2015/749837

Rauf, A., Jehan, N., Ahmad, Z., and Mubarak, M. S. (2017). "Analgesic potential of extracts and derived natural products from medicinal plants," in: *Pain Relief-From Analgesics to Alternative Therapies*, C. Maldonado (Ed.), InTechOpen, London, UK. https://doi.org/10.5772/intechopen.68631

Subrahmanyam, M., and Mohan, S. (2013). "Safety features in anaesthesia machine," *Ind. J. Anaes*. 57(5), 472-480. https://doi.org/10.4103/0019-5049.120143

Ullah, H., Samad, K., and Khan, F. A. (2014). "Continuous interscalene brachial plexus block *versus* parenteral analgesia for postoperative pain relief after major shoulder surgery," *Cochrane Db. Syst. Rev.* 2, article CD007080. https://doi.org/10.1002/14651858.CD007080.pub2

Witkin, L. B., Hubner, C. F., Galdi, F., O'Keefe, E., Spiletta, P., and Plummer, A. (1952). "Pharmacology of 2 amino indane hydro (SU 8629), a potent non narcotic analgesic," *J. Pharmacol. Exp. Ther*. 133(3), 400-408.

Zhang, J., Yang, H., Shen, G., Cheng, P., Zhang, J., and Guo, S. (2010). "Reduction of graphene oxide *via* L-ascorbic acid," *Chem. Commun*. 46, 112-114. https://doi.org/10.1039/b917705a

Article submitted: October 1, 2024; Peer review completed: December 19, 2024; Revised version received: October 30, 2025; Accepted: December 18, 2025; Published: December 29, 2025.
DOI: 10.15376/biores.21.1.1429-1442